Interaction of Hydrophobically End-Capped Poly(ethylene glycol) with Phospholipid Vesicles: The Hydrocarbon End-Chain Length Dependence

Fang Zhao, Xinxin Cheng, Guangming Liu, and Guangzhao Zhang*

Hefei National Laboratory for Physical Sciences at Microscale, Department of Chemical Physics, University of Science and Technology of China, Hefei, People's Republic of China

Received: October 20, 2009; Revised Manuscript Received: December 2, 2009

We have investigated the adsorption of hydrophobically end-capped poly(ethylene glycol) (HE-PEG) with carbon number (m) in the hydrocarbon end chain ranging from 0 to 16 onto phospholipid membrane by use of quartz crystal microbalance with dissipation (QCM-D), surface plasmon resonance (SPR) and isothermal titration calorimetry (ITC). QCM-D and SPR studies show that the hydrophobic interaction between HE-PEG chains and the lipid membrane increases with the hydrocarbon chain length. At a low HE-PEG concentration, the adsorption cannot induce a vesicle-to-bilayer transition until the carbon number is up to 16. However, at a high HE-PEG concentration, the adsorption results in a vesicle-to-bilayer transition at $m \geq 12$. ITC measurements demonstrate that enthalpy change (ΔH) for the mixing of lipid vesicles with HE-PEG chains is too small to be detectable when m is less than 12. However, ΔH changes from positive to negative as the carbon number increases from 12 to 16, indicating that the HE-PEG insertion increases with its hydrocarbon end-chain length. The present study reveals that the hydrophobic interaction between the lipid membrane and HE-PEG chains as well as the osmotic pressure drive the adsorption and insertion of such polymer chains.

Introduction

Phospholipid vesicles or liposomes are often used as simplified model systems for the biological cell because they are composed of similar materials, that is, phospholipid molecules.[1–3] Liposomes with such unique properties are expected to be promising carriers for drug delivery and gene transfection.[4–6] However, they usually have a short circulation time in bloodstream due to their poor stability, which limits such applications in practice.[7,8] It is reported that liposomes can be sterically stabilized by biocompatible polymers such as poly(ethylene glycol) (PEG) chemically or physically attached on them.[9,10] In principle, the adsorption and binding of nonionic polymers on liposomes via hydrophobic anchor groups can protect liposomes from nonspecific uptake by the reticuloendothelial system.[11] Considering that liposomes are made of a number of amphiphilic phospholipid molecules,[12–18] the fundamental issue related to the binding of polymer chains onto the vesicle surface is the hydrophobic interaction between the anchoring groups and the hydrophobic tails in the lipid bilayer. Actually, our previous work reveals that the hydrophobic end group in PEG profoundly influences its interaction with a lipid membrane.[18] However, the exact relation between the hydrocarbon end-chain length and polymer−liposome interaction is not clear yet.

On the other hand, many life processes ranging from membrane fusion to viral infection are mediated by the hydrophobic interactions between the proteins and the biomembranes.[19–22] It is generally accepted that the mismatch between the hydrophobic thickness of lipid bilayer and the hydrocarbon length of the integral membrane proteins play the most important role in lipid−protein interaction.[19] Without a good match, the proteins would not incorporate into biomembranes.[20] To reduce the hydrophobic mismatch, either the structure of membrane protein or the lipid bilayer has to be altered.[21] In addition, the insertion efficiency increases with the length of hydrophobic segment of the protein when the hydrophobic length of integral protein is less than the lipid bilayer hydrophobic thickness.[22] Therefore, the study on the interaction of polymers with liposome membrane can also help us to understand the membrane-related life processes.

In the present study, we have prepared hydrophobically end-capped PEG (HE-PEG) samples with hydrocarbon end chain different in length and investigated their interaction with lipid vesicles by use of quartz crystal microbalance with dissipation (QCM-D), surface plasmon resonance (SPR), as well as isothermal titration calorimetry (ITC). Our aim is to understand the role of hydrocarbon end-capped chain length in the liposome/HE-PEG interaction.

Experimental Section

Materials. Monohydroxy poly(ethylene glycol) ($HO(CH_2CH_2O)_{57}CH_3$) from BASF was vacuum-dried prior to use. Its molecular weight (M_w) determined by gel permeation chromatography (GPC) is 2.55×10^3 g/mol. Alkyloyl chloride with hydrocarbon chain different in length (98%) from Nanjing Chemlin Chemical Industry Co. was used as received. A hydrophobically end-capped PEG ($CH_3(CH_2)_{m-2}COO(CH_2CH_2O)_{57}CH_3$) was prepared by coupling PEG with alkyloyl chloride through acylation reaction. Typically, after butyl chloride (500 uL) was dissolved in toluene (10 mL) in a 100 mL three-necked flask, PEG (3.0 g) in toluene (20 mL) was slowly added. The reaction was allowed to proceed for 6 h at 90 °C, and then the solution was added into petroleum ether dropwise yielding white precipitate, which was filtered and washed with petroleum ether. Finally, the product was dried in a vacuum oven at 40 °C for 24 h. The yield was 90% determined by ^{1}H NMR. L-α-phosphatidylcholine (Aldrich, 99%) was from egg yolk. The buffer used was 10 mM Tris (100 mM NaCl, pH 8.0). Milli-Q water was used to prepare buffer solution.

* To whom correspondence should be addressed.

10.1021/jp910024n
Published on Web 12/31/2009

Preparation of Lipid Vesicles. The details about the preparation of small unilamellar vesicles (SUVs) can be found elsewhere.[18] Briefly, a certain mass of L-α-phosphatidylcholine was dissolved in chloroform, and the mixture was dried onto the wall of a continuously rolled flask under flowing N_2. Such formed thin film was exposed to high vacuum to remove the solvent completely. After the dried film was dispersed in Tris buffer under N_2 atmosphere, it was sonicated for ~60 min in a Scientz sonicator (Ningbo Scientz Biotechnology Co.) until a clear solution was resulted. The sample was sonicated in an ice/water mixture and the sonication and cooling were alternatively performed, that is, the sample was cooled for 5 s after every 5 s of sonication, in case that the sample was destroyed by heating. Titanium particles from the sonicator tip were removed by a centrifuge. The average hydrodynamic radius ($\langle R_h \rangle$) of the SUVs measured by dynamic laser light scattering (DLS) on an ALV-5022F spectrometer is ~30 nm. The average molecular weight of L-α-phosphatidylcholine measured by a combination of elemental analysis and mass spectrometer is 818 g/mol with an average carbon number of 18 in its tail.

QCM-D Measurements. The measurements were performed on a QCM-D (Q-sense AB) having an AT-cut crystal with fundamental resonant frequency of 5 MHz and mass sensitivity constant of 17.7 ng/cm^2 Hz. The crystal was mounted in a fluid cell with one side exposed to the solution.[23] In principle, a quartz crystal is excited to oscillate in the thickness shear mode at its fundamental resonant frequency (f_0) when a RF voltage near the resonant frequency is applied across the electrodes. A decrease in resonant frequency (Δf) proportional to the mass change (Δm) of the layer is resulted when a small layer is added to the electrodes. In vacuum or air, if the added layer is rigid, evenly distributed, and much thinner than the crystal, Δf is related to Δm and the overtone number ($n = 1, 3, 5.. ..$) by the Sauerbrey equation[24]

$$\Delta m = \frac{\rho_q l_q}{f_0}\frac{\Delta f}{n} \tag{1}$$

where f_0 is the fundamental frequency, and ρ_q and l_q are the specific density and thickness of the quartz crystal, respectively. The dissipation factor (D) defined by $D = E_d/2\pi E_s$ with E_d and E_s being the energy dissipated during one oscillation and the energy stored in the oscillating system is measured based on the fact that the voltage over the crystal decays exponentially as a damped sinusoidal when the driving power of a piezoelectric oscillator is switched off.[23] By switching the driving voltage on and off periodically, we can simultaneously obtain a series of changes of the resonant frequency (Δf) and the dissipation factor (ΔD). Δf and ΔD values from the fundamental overtone were usually noisy because of insufficient energy trapping and thus discarded.[25] Here, we only presented the data from the third overtone ($n = 3$) since it has a larger penetration depth of acoustic wave than the fifth ($n = 5$) and seventh overtones ($n = 7$).

The gold-coated resonator was cleaned by using Piranha solution composed of one part H_2O_2 and three parts H_2SO_4 for 15 min at 70 °C, rinsed with Milli-Q water, and blown dry with N_2 before use. The SiO_2-coated resonator was cleaned by exposing to UV-produced ozone in air for 30 min followed by immersing into 2% sodium dodecyl sulfate (SDS) solution for 10 min of sonication. The resonator was rinsed with Milli-Q water and dried under N_2. In the experiments about the adsorption of HE-PEG on lipid membrane, a rinsing with Tris buffer was done to remove unabsorbed polymer chains after the adsorption for each sample. All measurements were conducted at 25 ± 0.02 °C with Tris buffer as the reference.

SPR Measurements. SPR measurements were carried out on Biacore X at 25 °C with Tris buffer as the reference. The gold-coated glass plate was attached to a glass prism ($n \approx 1.65$) with a silicone opto-interface between them so that they matched in refractive index.[26,27] In principle, light from a near-infrared light-emitting diode focuses on to the sensor surface in a wedge-shaped beam through the prism to give a fixed range of incident light angle. Light reflected from the sensor is monitored by a linear array of light-sensitive diodes with a resolution of ~0.1°. The SPR response is linearly related to the mass of the added layer with 1000 RU ≈ 1 ng/ mm^2, where RU is the response unit.[28] The HE-PEG solution was delivered to the lipid vesicle surface at a flow rate of 10 μL/min within 10 min. Then the lipid vesicle surface was rinsed with Tris buffer to remove unabsorbed HE-PEG chains. The adsorption quantity of HE-PEG designated as the change of RUs (ΔRU) was obtained by subtracting the RU value for Tris buffer.

ITC Measurements. ITC experiments were carried out on a VP-ITC titration calorimeter (MicroCal) at 25 °C with deionized water as the reference. Each solution was thoroughly degassed to remove bubbles before loading. HE-PEG solution (0.1 mg/ mL) was placed in a continuously stirred syringe. Titration was performed by injecting 10 μL aliquots of lipid vesicle (6 mg/ mL) in Tris buffer into the calorimeter cell containing HE-PEG solution at an interval of 2 min. To minimize the error associated with diffusion from the syringe during baseline equilibration, the first injection was set to 8 uL and the associated heat was not included in the data analysis. The data for the titration of lipid vesicle into pure buffer as the baseline was subtracted from the raw data to correct the heat of dilution. Data analysis was done by use of the supplied software from MicroCal. The titration was analyzed according to the equation, P + L = PL; as a result, the chemical equilibrium can be written as

$$K = \frac{C_{PL}}{C_P C_L} = \frac{C_{PL}}{(C^0_{P_0} - C_{PL})(C^0_L - C_{PL})} \tag{2}$$

where P and L denote PEG chains and lipid vesicles, respectively, and C is the concentration, K is the binding constant. The total heat (h) adsorbed or released after i injections is

$$\sum_i h_i = \Delta H C^i_{PL} V_{cell} \tag{3}$$

where ΔH is the enthalpy change during the binding, and V_{cell} is the volume of the reaction vessel. By the combination of eqs 2 and 3, ΔH and K can be obtained by fitting the titration curve using a nonlinear least-squares minimization method with some adjustable parameters (Levenberg−Marquardt algorithm) as reported before.[29] One set of sites or two set of sites model was applied for the data fitting depending on the curves. The free energy change (ΔG) and the entropy change (ΔS) were estimated from the following equations:

$$\Delta G = -RT \ln K \tag{4}$$

$$\Delta G = \Delta H - T\Delta S \tag{5}$$

Results and Discussion

We first examined the adsorption of lipid vesicles on different surfaces. Figure 1a shows the typical changes in frequency (Δf)

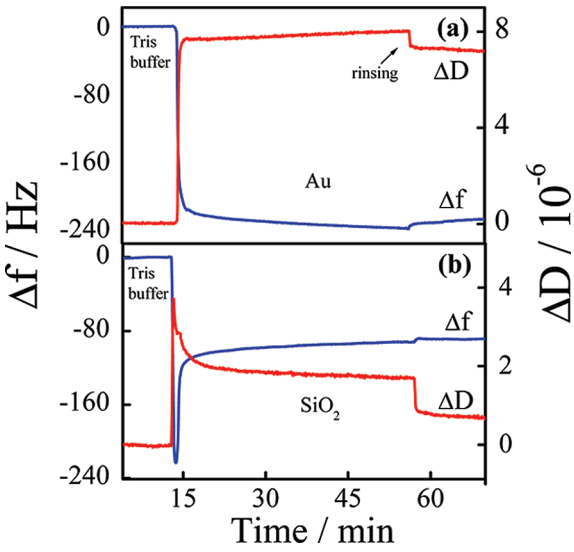

Figure 1. The changes in frequency (Δf) and dissipation (ΔD) as a function of time for the adsorption of lipid vesicles on different surfaces, where the concentration of lipid vesicle is 3.0 mg/mL.

SCHEME 1: Illustration for the Morphologies of the Adsorbed Lipid Vesicles on Gold Surface and the Solid-Supported Lipid Bilayer on SiO_2 Surface

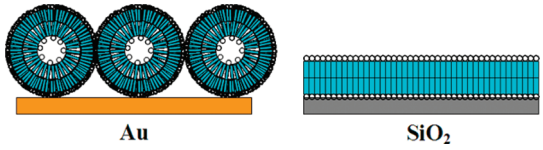

and dissipation (ΔD) as a function of time for the adsorption of lipid vesicles onto a gold-coated resonator surface. Δf decreases and ΔD increases rapidly in the initial stage and then gradually level off, indicating the saturation of lipid vesicles on the surface. The monotonic changes in Δf and ΔD demonstrate that the lipid vesicles absorbed on the gold surface are intact. In contrast, the adsorption of lipid vesicles onto a SiO_2-coated resonator surface looks quite different (Figure 1b). Δf first decreases and then increases with a minimum, while ΔD exhibits an opposite behavior with a maximum in the adsorption isotherm. As reported before,[18,30] it is an indicative of a vesicle-to-bilayer transition. Namely, the adsorbed lipid vesicles form a continuously solid-supported lipid bilayer (s-SLB) on the SiO_2 surface. Scheme 1 illustrates the morphologies of SUVs on the two kinds of surface.

Figure 2 shows the changes in frequency (Δf) and dissipation (ΔD) as a function of time for the adsorption of HE-PEG onto the s-SLB surface formed on the SiO_2 coated resonator surface. Here, the concentration of HE-PEG is 0.1 mg/mL. From the DLS measurements conducted in our preliminary experiments, HE-PEG chains do not form aggregates but exist as individual chains at this concentration. HE-PEG with m carbons in the hydrocarbon end chain is designated as Cm in the figures thereafter. When the carbon number $m = 11$, the introduction of HE-PEG solution does not induce any significant change in either Δf or ΔD, suggesting a slight adsorption of HE-PEG chains on the s-SLB surface. Particularly, both Δf and ΔD return to the baselines after rinsing, further indicating that very few HE-PEG chains are adsorbed on the s-SLB surface, that is, the lipid bilayer only has a very weak interaction with HE-PEG chains. Actually, our preliminary experiments demonstrate that HE-PEG chains do not adsorb on the lipid bilayer surface in the range of m from 0 to 11 (data not shown). However, Δf

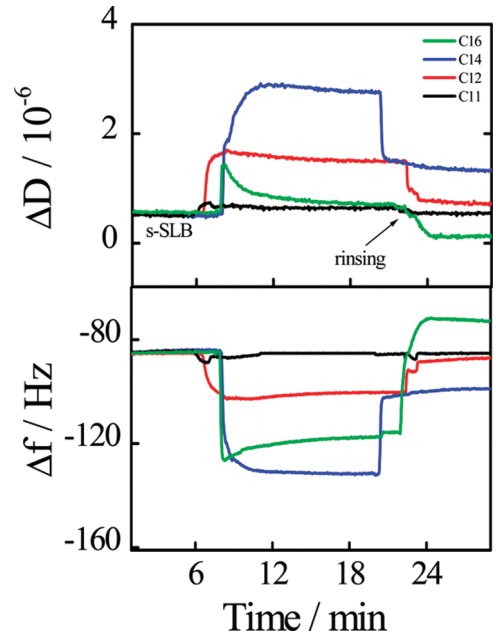

Figure 2. The changes in frequency (Δf) and dissipation (ΔD) as a function of time for the adsorption of HE-PEG chains onto the s-SLB surface, where the HE-PEG concentration is 0.1 mg/mL. HE-PEG with m carbons in the hydrocarbon end chain is designated as Cm thereafter.

decreases and ΔD increases significantly when the carbon number reaches 12. Since the viscosity and density of HE-PEG solution is close to that of the buffer at such a low concentration, the changes in Δf and ΔD are attributed to the attachment of HE-PEG chains onto the s-SLB surface. Both Δf and ΔD almost return to the baselines after rinsing, implying that most HE-PEG chains are removed from the lipid bilayer. This is because the hydrophobic interaction between HE-PEG and lipid bilayer is not strong enough to suppress the impact of the rinsing at $m = 12$. When m increases to 14, Δf and ΔD exhibit a large change even after the rinsing, indicating that the hydrophobic interaction becomes so strong that some HE-PEG chains root in lipid bilayer and cannot be removed upon rinsing. When m increases to 16, a more complex behavior can be observed. Δf and ΔD exhibit a minimum and a maximum in the adsorption isotherm, respectively. The initial decrease of Δf and increase of ΔD can be attributed to the deep insertion of HE-PEG chains in the lipid bilayer and the association of the inserted chains with the incoming chains on the membrane surface. Note that HE-PEG chains can form aggregates on the membrane surface even at the concentration below CMC.[31] Subsequently, Δf increases and ΔD decreases slowly, indicating that the trapped water molecules in the HE-PEG aggregates are slowly released out due to the rearrangement of HE-PEG chains on the membrane surface. After rinsing, Δf is higher than the baseline and ΔD is lower than the baseline, indicating that the HE-PEG aggregates and some associated phospholipid molecules are removed from the membrane surface.[32] Similar results have also been observed for the adsorption of HE-PEG chain with 18 carbons in the hydrocarbon end-chain.[18] Considering that the hydrophobic interaction between HE-PEG chains and lipid bilayer increases as the length of the hydrocarbon end chain increases, the adsorption and insertion of HE-PEG chains on the lipid membrane surface is driven by the hydrophobic interaction.

Actually, the binding of HE-PEG chains on lipid membrane is mediated by the hydrophobic attraction between the hydrocarbon end chain and the hydrophobic tail of lipid as well as

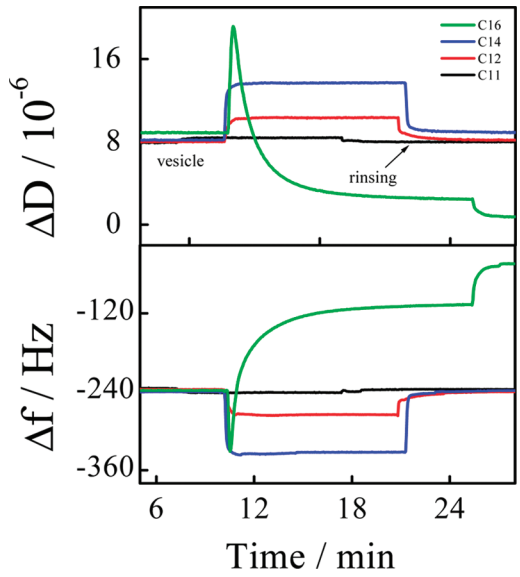

Figure 3. The changes in frequency (Δf) and dissipation (ΔD) as a function of time for the adsorption of HE-PEG chains onto the layer formed by lipid vesicles, where the HE-PEG concentration is 0.1 mg/mL.

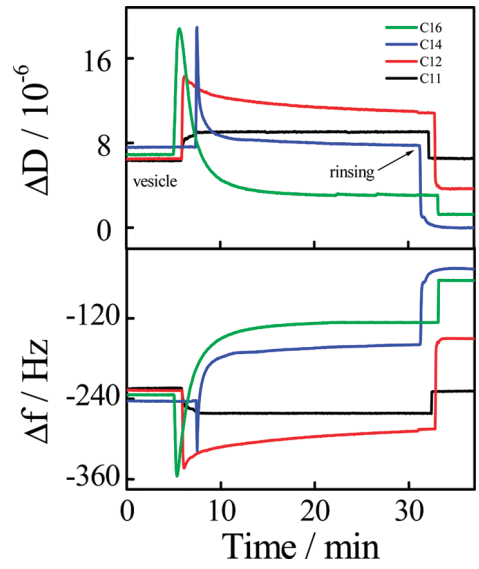

Figure 4. The changes in frequency (Δf) and dissipation (ΔD) as a function of time for the adsorption of HE-PEG chains onto the layer formed by lipid vesicles, where the HE-PEG concentration is 2.0 mg/mL.

the steric repulsion between PEG chains. When the former dominates the later, HE-PEG chains would bind onto the lipid membrane. In the present study, the binding is mediated by the former because the length of the hydrophilic PEG chain is fixed. Clearly, the critical value of carbon number in the hydrocarbon end chain is 12, above which the hydrophobic end chain can insert into the lipid bilayer. In other words, the hydrocarbon end chain can insert into the lipid membrane when its length is up to about one-third of the hydrophobic wall thickness of lipid bilayer with 36 carbon atoms. On the other hand, the rinsing would produce a shear force driving the PEG chains away from the membrane surface if the hydrophobic attraction is not strong enough. This explains why both Δf and ΔD can return to the baselines after rinsing when the hydrocarbon end chain is not long enough. Note that the polymer aggregates would undergo a much larger shear force during rinsing compared with individual chains so that they can be removed from the membrane surface at $m = 16$.

After examining the adsorption of HE-PEG chains on the s-SLB surface, we have investigated the adsorption of HE-PEG chains onto the layer of lipid vesicles formed on the gold-coated resonator surface, which has a more complex structure relative to the s-SLB. The concentration of HE-PEG used here is also 0.1 mg/mL. Figure 3 shows that the introduction of HE-PEG to lipid vesicles does not lead to any obvious change in either Δf or ΔD at $m = 11$. Similar results have also been obtained for $m < 11$ (data not shown). However, Δf decreases and ΔD increases markedly when m increases to 12, indicating an adsorption of HE-PEG chains onto the lipid vesicle surface. Δf and ΔD almost return to the baselines after rinsing, implying that such a adsorption is weak and the adsorbed chains can be removed upon rinsing. Similar phenomena can also be observed at $m = 14$ except that ΔD is slightly higher than the baseline after rinsing, suggesting that the adsorption is some stronger than that for $m = 12$. When m increases to 16, Δf first sharply decreases and then rapidly increases with a minimum, whereas ΔD exhibits an opposite behavior with a maximum. This is similar to the vesicle-to-bilayer transition observed on the SiO_2 surface (Figure 1b). As revealed in Figure 2, HE-PEG chains can insert into the lipid membrane when the hydrophobic interaction between polymer chains and lipid bilayer is strong enough. Actually, the insertion of HE-PEG chains alters the vesicle curvature and the hydrophobic−hydrophilic interaction balance for stabilization of the vesicle,[18,33–35] so that the lipid vesicles rupture and fuse into a bilayer. The final Δf value after the rinsing is higher than the baseline, indicating that water molecules trapped in the vesicles are released out after the vesicle-to-bilayer transition. At the same time, ΔD after the rinsing is lower than the baseline, further indicating the transition from soft vesicles to a bilayer.

We have also examined the adsorption of HE-PEG chains at a higher concentration (2.0 mg/mL). In Figure 4, Δf decreases and ΔD increases after the introduction of HE-PEG solution at $m = 11$, indicating that the HE-PEG chains can adsorb on the vesicle surface at such a high concentration. Both Δf and ΔD return to the baselines after rinsing, implying that the adsorption is weak and the adsorbed chains can be removed by rinsing. However, only small changes in Δf and ΔD can be observed upon the introduction of HE-PEG chains when m is less than 11 (data not shown), which are due to the small differences in density and viscosity between HE-PEG solution and the Tris buffer. When m increases to 12, Δf and ΔD show a minimum and a maximum, respectively, indicating that lipid vesicles rupture and fuse into a bilayer due to the adsorption and insertion of HE-PEG chains. This is in contrast with the case at the concentration of 0.1 mg/mL, where HE-PEG chains cannot induce the rupture of vesicles but only weakly attach on the membrane surface (Figure 3). The reason is that the adsorption and insertion of HE-PEG chains are not only related to the hydrophobic interaction but also to the osmotic pressure between the vesicle core and the HE-PEG solution outside the vesicle. As HE-PEG concentration increases, the osmotic pressure increases, promoting the insertion of HE-PEG chains into lipid vesicle membrane and accelerating the lipid vesicle disturbance. Moreover, HE-PEG chains form micelles at 2.0 mg/mL, which further increases the local concentration of HE-PEG chains near the vesicle surface when the micelles are adsorbed on the membrane surface. Likewise, a vesicle-to-bilayer transition also happens at such a high HE-PEG concentration at $m = 14$. Thus, the combination of hydrophobic interaction and osmotic pressure

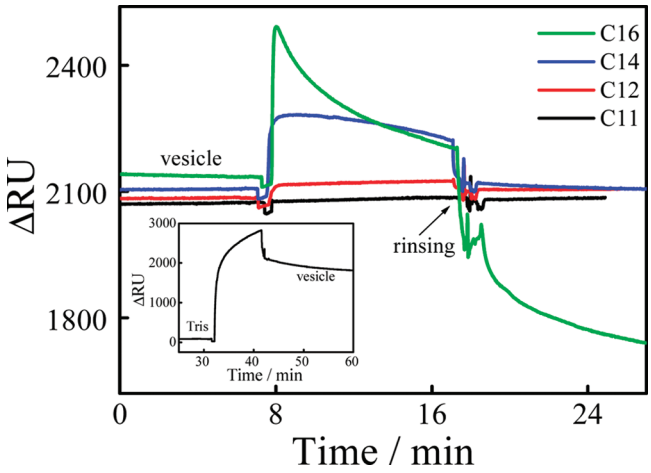

Figure 5. SPR sensorgrams for the adsorption of HE-PEG chains onto the gold-supported lipid vesicles, where the HE-PEG concentration is 0.1 mg/mL.

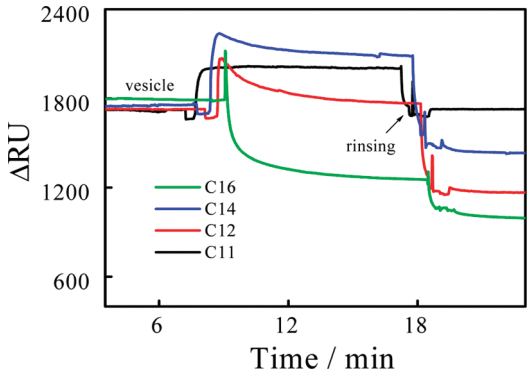

Figure 6. SPR sensorgrams for the adsorption of HE-PEG chains onto the gold-supported lipid vesicles, where the HE-PEG concentration is 2.0 mg/mL.

leads to the vesicle-to-bilayer transition. Similar results are also obtained at $m = 16$.

Figure 5 shows the SPR sensorgrams for the adsorption of HE-PEG chains onto the gold-supported lipid vesicles, where the HE-PEG concentration is 0.1 mg/mL. The quick increase in SPR signal shown in the inset indicates the adsorption of lipid vesicles onto the gold surface. The rinsing with buffer leads to a small decrease in the SPR response (ΔRU) implies the removal of some excessive vesicles upon rinsing. Subsequently, the HE-PEG solution is introduced into the cell. ΔRU slightly increases at $m = 11$, indicating the weak interactions between HE-PEG chains and lipid vesicles. Similar phenomena are also observed when m is less than 11 (data not shown). When m is in the range from 12 to 14, ΔRU increases after the addition of HE-PEG chains but returns to the baseline after rinsing, indicating that HE-PEG chains with longer hydrocarbon end chain can adsorb on the vesicle surface, and they can be removed by rinsing. When m increases to 16, much stronger hydrophobic interaction between HE-PEG chains and vesicle membrane is expected. Thus, ΔRU exhibits a maximum in the adsorption isotherm, which is much lower than the baseline after rinsing. The facts indicate a vesicle-to-bilayer transition due to the gradual insertion of HE-PEG chains into the vesicle membrane. This is consistent with the QCM-D results shown in Figure 3.

Figure 6 shows SPR sensorgrams for the adsorption of HE-PEG chains onto gold-supported lipid vesicles, where the HE-PEG concentration is 2.0 mg/mL. ΔRU first increases and returns to the baseline after rinsing at $m = 11$, indicating that

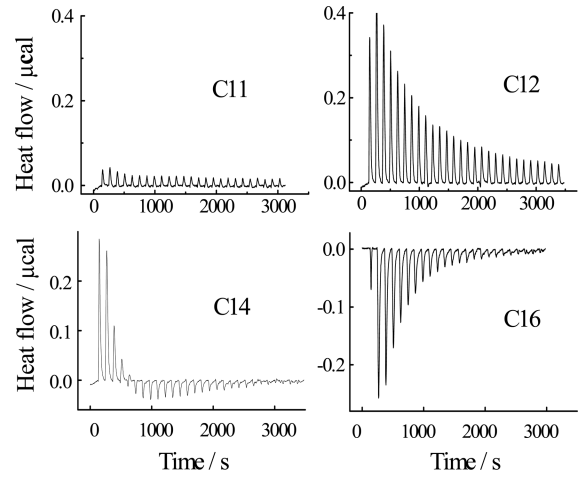

Figure 7. ITC curves for the raw titration measurement of HE-PEG solutions with lipid vesicles. Each peak corresponds to the injection of 10 μL of lipid vesicle suspension (6.0 mg/mL) into HE-PEG solution (0.1 mg/mL).

TABLE 1: Thermodynamic Parameters for the Interaction of HE-PEG Chains and Lipid Vesicles

HE-PEG	ΔH kcal/mol	$T\Delta S$ kcal/mol	ΔG kcal/mol
C0−C11	0	0	0
C12	0.42	5.13	−4.71
C14[a]	0.67	6.86	−6.19
C14[b]	−0.09	4.62	−4.71
C16	−0.20	5.16	−5.36

[a] For the endothermic peak. [b] For the exothermic peak.

the adsorbed HE-PEG chains can be removed by the rinsing and no vesicle-to-bilayer transition occurs during the adsorption. However, ΔRU exhibits a maximum in the adsorption isotherm and the ΔRU value after the rinsing is lower than the baseline as observed in the QCM-D experiments (Figure 4) when $m \geq 12$, suggesting that HE-PEG chains with longer hydrocarbon end chain can adsorb and insert into the vesicle membrane driven by the combination of the hydrophobic interaction and the osmotic pressure, resulting in a vesicle-to-bilayer transition.

To understand the interactions between HE-PEG chains and lipid vesicles, we have also investigated the energy change regarding the interactions between HE-PEG and lipid vesicles. Figure 7 shows ITC curves for the raw titration measurement of HE-PEG solutions with lipid vesicles. All titrations were performed below CMC of HE-PEG to eliminate the solubilization effect.[36] Each peak represents the heat associated with the interaction between HE-PEG chains and lipid vesicles. Only a small dilution heat is observed upon introduction of lipid vesicles into HE-PEG solution at $m = 11$, indicating a very weak interaction between HE-PEG chains and the lipid vesicles. Similar results are also obtained at $m < 11$ (data not shown). An obvious endothermic peak is observed at $m = 12$. This is understandable because the hydrophobic interaction between HE-PEG chains and the lipid vesicles increases with the hydrocarbon end-chain length. As the amount of vesicles in the sample cell increases, the free HE-PEG chains available for partition decrease, thus the heat flow decreases and levels off. Table 1 shows that both the enthalpy change (ΔH) and entropy change (ΔS) are positive at $m = 12$. This is because the lateral compression in the polar region of lipid bilayer results in dehydration of HE-PEG chains.[36–40] Namely, when HE-PEG chains transfer from bulk phase to vesicle membrane surface, the dehydration leads to a positive ΔH. On the other hand, the

release of water into bulk solution gives rise to a gain in entropy, which acts as the main driving force for the lipid membrane partitioning ($\Delta G < 0$). ITC curve for $m = 14$ is more complex. An endothermic peak can be observed at the early stage, similar to that at $m = 12$. Later, such an endothermic peak vanishes. Instead, a small exothermic peak comes out. The facts indicate two interactions compete in the adsorption of HE-PEG chains, which oppositely contribute to ΔH. When $m = 16$, only exothermic peaks can be observed, that is, ΔH for the adsorption of HE-PEG on lipid vesicles are negative. This is due to the strong hydrophobic interaction between the hydrocarbon chains of HE-PEG and lipid membrane.[40,41] Note that the deep insertion of the HE-PEG chains expands the lipid membrane and improves the chain motion fluidizability,[41–45] which requires an additional surface hydration. The rehydration effect yields a negative ΔH. In other words, HE-PEG weakly adsorbs on the lipid membrane at $m = 12$, and the dehydration of HE-PEG chains upon attachment to lipid membrane leads to a positive ΔH. When $m = 14$, HE-PEG can insert into lipid membrane. The initial attachment of PEG chains onto the lipid membrane leads to a positive ΔH due to the dehydration of PEG chains, whereas the following rehydration of PEG chains results in a negative ΔH because of the expansion of lipid membrane. Therefore, two opposite contributions to ΔH can be observed at $m = 14$. When $m = 16$, HE-PEG chains deeply insert into lipid membrane, the enthalpy change is mainly comes from the rehydration so that ΔH is negative. In other words, as the hydrocarbon end-chain length increases, both enthalpy and entropy would contribute to the free energy change. Additionally, it seems that enthalpy change determines the interaction of modified PEG and lipid membrane since the entropy changes were similar for all PEGs with various hydrophobic end chains (Table 1).

Conclusion

The adsorption of hydrophobically end-capped poly(ethylene glycol) with carbon number (m) in the hydrocarbon end chain ranging from 0 to 16 onto phospholipid membrane has been investigated by use of quartz crystal microbalance with dissipation, surface plasmon resonance, and isothermal titration calorimetry. Lipid vesicles adsorbed on the SiO_2 surface form solid-supported lipid bilayer but retain intact vesicles on the gold surface. The hydrophobic interaction between the HE-PEG chains and lipid membrane increases with the hydrocarbon end-chain length of HE-PEG chains. At a low HE-PEG concentration, the adsorption does not induce a vesicle-to-bilayer transition until m reaches 16. However, at a high HE-PEG concentration, the adsorption results in such a transition at $m \geq 12$ due to the combination of hydrophobic interaction and osmotic pressure. The ability of HE-PEG to insert in a lipid vesicle increases with its hydrocarbon end-chain length.

Acknowledgment. The financial support of the National Distinguished Young Investigator Fund (20474060), Ministry of Science and Technology of China (2007CB936401) and State Key Lab of Polymer Physics and Chemistry (Changchun) is acknowledged.

References and Notes

(1) Cevc, G.; Richardsen, H. *Adv. Drug Delivery Rev.* **1999**, *38*, 207.
(2) Lasic, D. D.; Needham, D. *Chem. Rev.* **1995**, *95*, 2601.
(3) Sun, J. J.; Vernier, G.; Wigelsworth, D. J.; Collier, R. J. *J. Biol. Chem.* **2007**, *282*, 1059.
(4) Sharma, A.; Sharma, U. S. *Int. J. Pharm.* **1997**, *154*, 123.
(5) Torchilin, V. P.; Trubetskoy, V. S. *Adv. Drug Delivery Rev.* **1995**, *16*, 141.
(6) Marjan, J. M. J.; Allen, T. M. *Biotechnol. Adv.* **1996**, *14*, 151.
(7) Woodle, M. C.; Storm, G. Long Circulating Liposomes: Old Drugs, New Therapeutics; Springer: Germany, 1998.
(8) Barenholz, Y. *Curr. Opin. Colloid Interface Sci.* **2001**, *6*, 66.
(9) Ringsdorf, H.; Schlarb, B.; Venzmer, J. *Angew. Chem., Int. Ed. Engl.* **1988**, *27*, 113.
(10) Sou, K.; Eudo, T.; Takeoka, S.; Tsuchida, E. *Bioconjugate Chem.* **2000**, *11*, 372.
(11) Tseng, Y. C.; Mozumdar, S.; Huang, L. *Adv. Drug Delivery Rev.* 2009.
(12) Ringsdorf, H.; Schlarb, B.; Venzmer, J. *Angew. Chem., Int. Ed.* **1988**, *27*, 113.
(13) Polozova, A.; Winnik, F. M. *Biochim. Biophys. Acta* **1997**, *1326*, 213.
(14) Maskarinec, S. A.; Hannig, J.; Lee, R. C.; Lee, K. Y. C. *Biophys. J.* **2002**, *82*, 1453.
(15) Firestone, M. A.; Wolf, A. C.; Seifert, S. *Biomacromolecules* **2003**, *4*, 1539.
(16) Firestone, M. A.; Seifert, S. *Biomacromolecules* **2005**, *6*, 2678.
(17) Liang, X. M.; Mao, G. Z.; Simon Ng, K. Y. *J. Colloid Interface Sci.* **2005**, *285*, 360.
(18) Liu, G. M.; Fu, L.; Zhang, G. Z. *J. Phys. Chem. B* **2009**, *113*, 3365.
(19) Venturoli, M.; Smit, B.; Sperotto, M. M. *Biophys. J.* **2005**, *88*, 1778.
(20) Harzer, U.; Bechinger, B. *Biochemistry* **2000**, *39*, 13106.
(21) Lee, A. G. *Biochim. Biophys. Acta* **2003**, *1612*, 1.
(22) Ridder, A. N. J. A.; van de Hoef, W.; Stam, J.; Kuhn, A.; de Kruijff, B.; Killian, J. A. *Biochemistry* **2002**, *41*, 4946.
(23) Rodahl, M.; Höök, F.; Krozer, A.; Kasemo, B.; Breszinsky, P. *Rev. Sci. Instrum.* **1995**, *66*, 3924.
(24) Sauerbrey, G. *Z. Phys.* **1959**, *155*, 206.
(25) Bottom, V. E. *Introduction to Quartz Crystal Unit Design*; Van Nostrand Reinhold Co.: New York, 1982.
(26) Kretschmann, E.; Raether, H. *Z. Naturforsch., A: Phys. Sci.* **1968**, *23*, 2135.
(27) Liedberg, B.; Nylander, C.; Lunstrom, I. *Sens. Actuators* **1983**, *4*, 299.
(28) Stenberg, E.; Persson, B.; Poss, H.; Urbaniczky, C. *J. Collioid Interface Sci.* **1991**, *143*, 513.
(29) Indyk, L.; Fisher, H. F. *Methods Enzymol.* **1998**, *295*, 350.
(30) Keller, C. A.; Kasemo, B. *Biophys. J.* **1998**, *75*, 1397.
(31) Ligoure, C. *Macromolecules* **1991**, *24*, 2968.
(32) Thid, D.; Benkoski, J. J.; Svedhem, S.; Kasemo, B.; Gold, J. *Langmuir* **2007**, *23*, 5878.
(33) Otten, D.; Lobbecke, L.; Beyer, K. *Biophys. J.* **1995**, *68*, 584.
(34) Lipowsky, R. *Phys. Rev. Lett.* **1996**, *77*, 1652.
(35) Tribet, C.; Vial, F. *Soft Matter* **2008**, *4*, 68.
(36) Heerklotz, H.; Lantzsch, G.; Binder, H.; Klose, G. *J. Phys. Chem.* **1996**, *100*, 6764.
(37) Heerklotz, H.; Binder, H.; Lantzsch, G.; Klose, G. *J. Phys. Chem. B* **1997**, *101*, 639.
(38) Trandum, C.; Westh, P.; Jørgensen, K.; Mouritsen, O. G. *J. Phys. Chem. B* **1999**, *103*, 4751.
(39) Nebel, S.; Ganz, P.; Seelig, J. *Biochemistry* **1997**, *36*, 2853.
(40) Heerklotz, H.; Wieprecht, T.; Seelig, J. *J. Phys. Chem. B* **2004**, *108*, 4909.
(41) Seelig, J.; Ganz, P. *Biochemistry* **1991**, *30*, 9354.
(42) Beschiaschvili, G.; Seelig, J. *Biochemistry* **1992**, *31*, 10044.
(43) Heerklotz, H.; Wieprecht, T.; Seelig, J. *J. Phys. Chem. B* **2004**, *108*, 4909.
(44) Heerklotz, H.; Binder, H.; Lantzsch, G.; Klose, G. *J. Phys. Chem. B* **1997**, *101*, 639.
(45) Thurmond, R. L.; Otten, D.; Brown, M. F.; Beyer, K. *J. Phys. Chem.* **1994**, *98*, 972.

JP910024N